substance: Sm_2S_3
property: crystal structure, physical properties

α-Sm_2S_3

crystal structure	orthorhombic (D_{2h}^{16} – Pnma)			
lattice parameters				
a	7.382(2) Å		color: red	68S
b	15.375(3) Å			
c	3.974(2) Å			
conductivity, Seebeck coefficient				
σ	6 Ω^{-1} cm^{-1}		(E_A = 0.001 eV)	68S
S	– 230 µV K^{-1}			68S

γ-Sm_2S_3

crystal structure	cubic (Th_3P_4-defect structure, T_d^6 – $I\bar{4}3d$)			
lattice parameters				
a	8.448 Å			60P
	8.43 Å			79C
	8.448 Å			85Z
melting point				
T_m	1780°C			60P
	1750°C			61H
linear thermal expansion coefficient				
α	$11.4 \cdot 10^{-6}$ K^{-1}			66D
energy gap and other energy parameters				
E_g	2.6 ± 0.1 eV		optical gap	85Z
	2.7 eV		X-ray spectra	83S
E_b	5.7 eV	S 3p-level	MgKα XPS, Fig. 6 (E_b rel. to E_F)	91K
	8 eV	Sm 4f-level	MgKα XPS, Fig. 6	
	14.8 eV	S 3s-level	MgKα XPS, Fig. 6	
	22.0 eV	Sm $5p_{3/2}$-level	MgKα XPS, Fig. 6	
	26.0 eV	Sm $5p_{1/2}$-level	MgKα XPS, Fig. 6	
	44 eV	Sm 5s-level	MgKα XPS, Fig. 6	
	134 eV	Sm $4d_{5/2}$-level	MgKα XPS, Fig. 7	
	137 eV	Sm $4d_{3/2}$-level	MgKα XPS, Fig. 7	
	249 eV	Sm ($4p_{3/2}$, $4p_{5/2}$)-lev.	MgKα XPS	
	1082 eV	Sm $3d_{5/2}$-level	AlKα XPS, Fig. 8	
	1109 eV	Sm $3d_{3/2}$-level	AlKα XPS, Fig. 8	

E	6.9 eV	S 3p-E_F	ELS, Fig. 9	91K
	10.5 eV	S 3p-cond. band, surface plasmon	ELS, Fig. 9	
	17.8 eV	bulk plasmon	ELS, Fig. 9	
	23.8 eV	Sm 5p-E_F	ELS, Fig. 9	
	32.1 eV	Sm 5p-5d	ELS, Fig. 9	
	≈ 50 eV	Sm 5s-E_F	ELS, Fig. 9	
conductivity				
σ	$< 10^{-9}$ Ω^{-1}cm^{-1}	near stoichiometric samples	reflectivity: Fig. 10; ε_1, ε_2, Im ε^{-1}: Fig. 11	83B
resistivity				
ρ	$7 \cdot 10^5$ Ω cm			65L

Further figures and references:

heat capacity [79C] and Fig. 1

coordination polyhedra: Fig. 2

photoconductivity spectra: Figs. 3...5

References:

60P Picon, M., Domange, L., Flahaut, J., Guittard, M., Patrie, M.: Bull. Soc. Chim. Fr. 2 (1960) 221.

61H Houston, M. D.: Rare Earth Research, Kleber, E. V. (ed.), New York: Mac Millan Comp. 1961, p. 255.

65L Lashkarev, G. V., Paderno, Yu. B.: Izv. Akad. Nauk SSSR, Neorg. Mater. 1 (1965) 1791.

66D Dudnik, E. M., Lashkarev, G. V., Paderno, Y. B., Obolonchik, V. A.: Inorg. Mater. 2 (1966) 833.

66H Holtzberg, F., Methfessel, S.: J. Appl. Phys. 37 (1966) 1433.

68S Sleight, A. W., Prewitt, C. T.: Inorg. Chem. 7 (1968) 2282.

79C Coey, J. M. D., Cornut, B., Holtzberg, F., von Molnar, S.: J. Appl. Phys. 50 (1979) 1923.

82G Glurdzhidze, L. N., Gzirishvili, D. G., Koshoridze, S. I., Dzhabua, Z. U., Sanadze, V. V.: Sov. Phys. Solid State 24 (1982) 795.

83B Balabanova, L.A., Zhuze, V.P., Ostroumova, E.G., Shul'man, S.G.: Sov. Phys. Solid State 25(6) (1983) 971.

83S Soldatov, A.V., Gusatinskii, A.N., Karin, M.G., Sidorin, K.K., Sadovskaya, O.A.: Inorg. Mater. 19 (1983) 951-954.

85Z Zhuze, V.P., Karin, M.G., Sidorin, K.K., Sokolov, V.V., Shelykh, A.I.: Sov. Phys. Solid State 27(12) (1985) 2205.

91K Kaciulis, S., Latisenka, A., Plesanovas A.: Surf. Sci. 251/252 (1991) 330.

Fig. 1.

γ-Sm_2S_3, Sm_3S_4, Sm_3Se_4. Temperature dependence of molar heat capacity. The increase below 7 K is explained by a Schottky anomaly due to the crystal field splitting (Δ_{cf} = 2.4 K) of Sm^{3+} [79C].

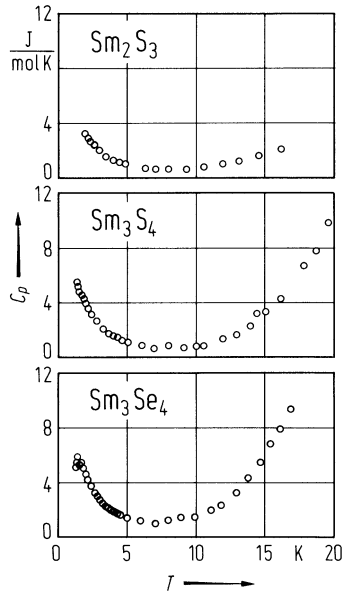

Fig. 2.

Th_3P_4-type compounds. The coordination polyhedra of the cations and the anions. Full circles: Th- atoms, other circles: P-atoms [66H].

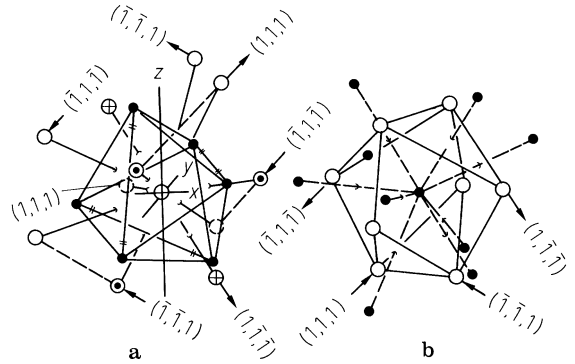

Fig. 3.

γ-Sm_2S_3:Cd. Photoconductivity spectra (relative change $\Delta\sigma/\sigma$ vs. photon energy) of a Cd-doped polycrystalline film at 115 K, 295 K, 384 K [82G].

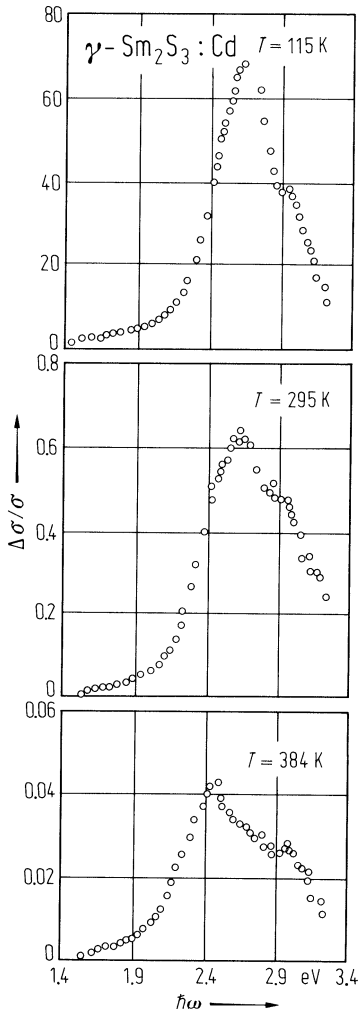

Fig. 4.

γ-Sm_2S_3:Pb,Cd. Photoconductivity spectra (photo emf vs. photon energy) of Pb-doped (*1*) and Cd- doped (*2*) films [82G].

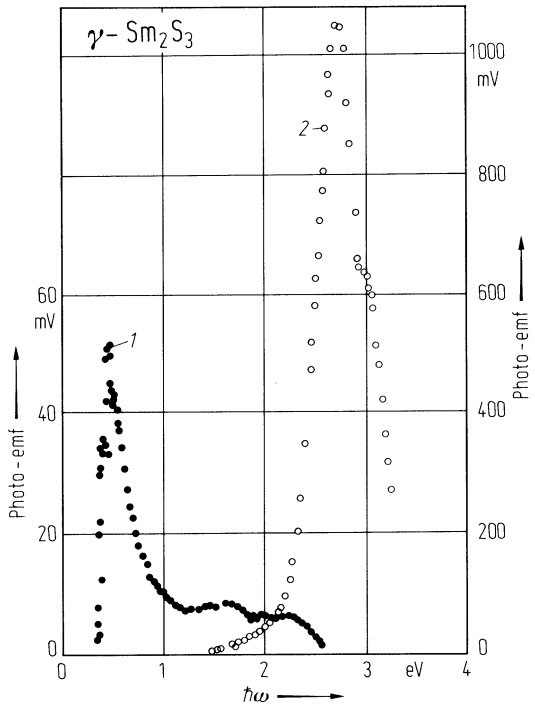

Fig. 5.

γ-Sm_2S_3:Pb. Fine structure of the photoconductivity spectrum (relative change $\Delta\sigma/\sigma$ vs. photon energy) of a Pb-doped film at 115 K, 190 K, and 300 K [82G].

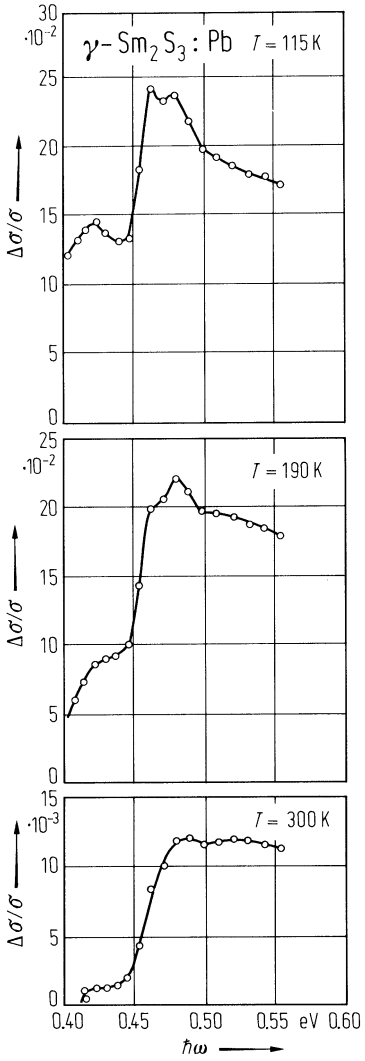

Fig. 6.

γ-Ln_2S_3. MgK_α X-ray photoelectron spectra of the rare-earth sesquisulfides (Ln = La, Ce, Nd, Sm, Gd, Dy) in the energy region below Fermi level down to Ln 5s core level [91K].

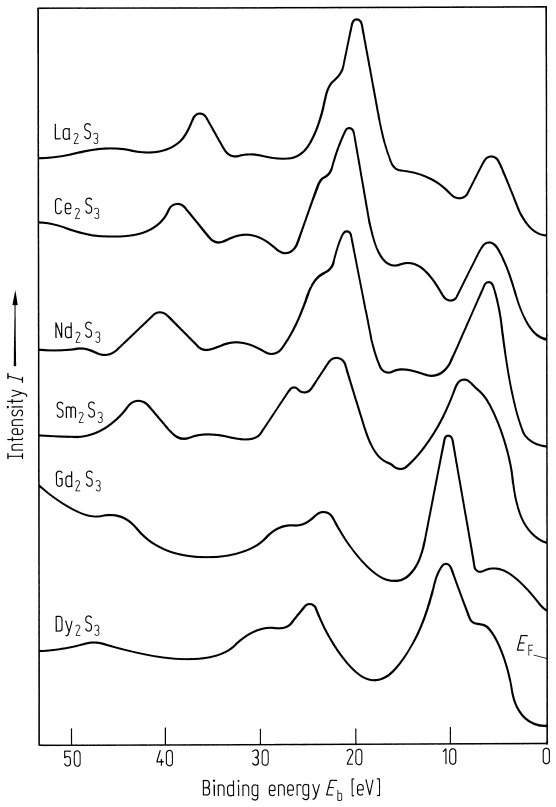

Fig. 7

γ-Ln_2S_3. MgK_α X-ray photoelectron spectra of the rare-earth sesquisulfides (Ln = La, Ce, Nd, Sm, Gd, Dy) in the 4d core level region [91K]. E_b relative to E_F.

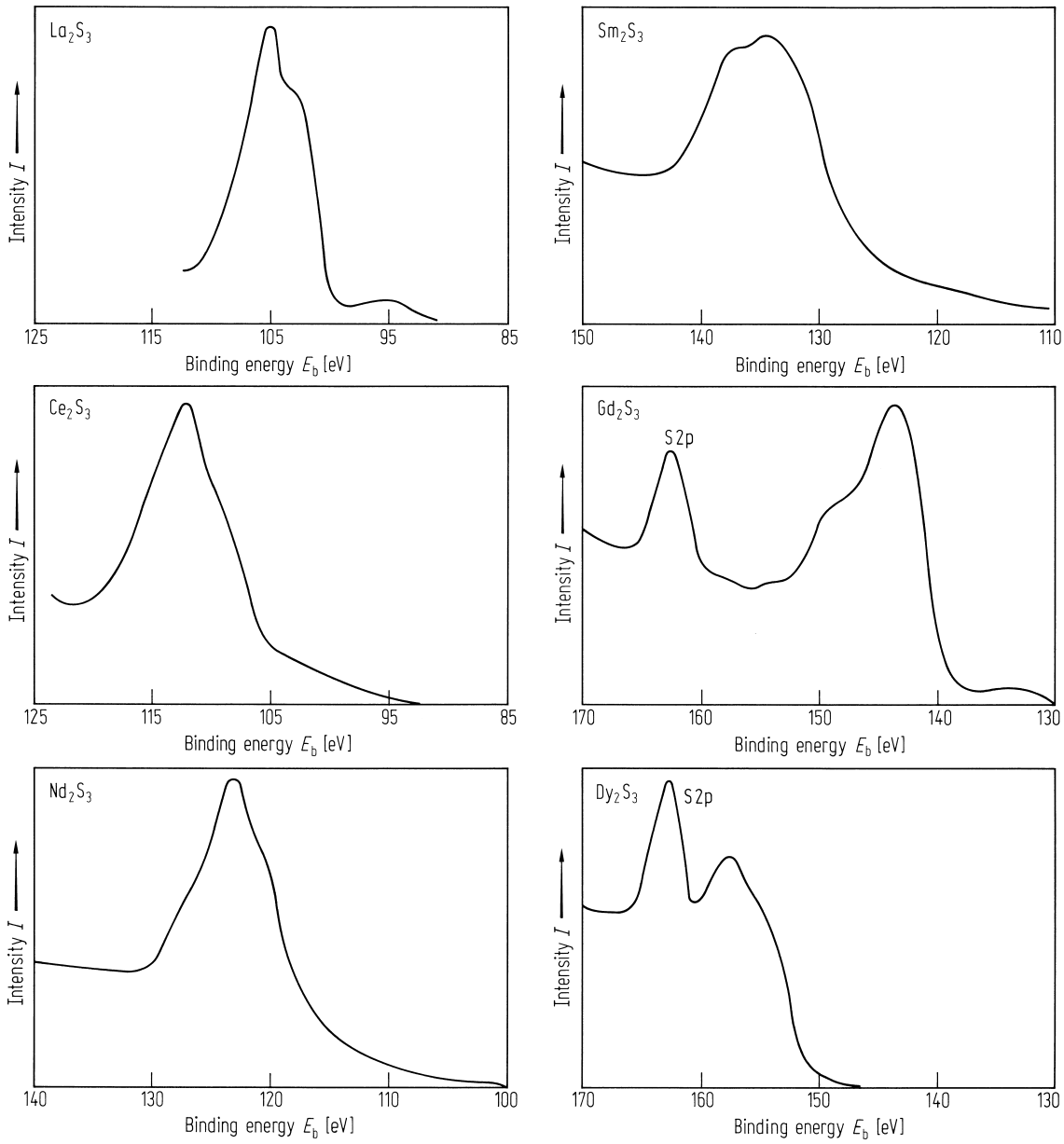

Fig. 8.

γ-Ln_2S_3. AlK_α X-ray photoelectron spectra of the rare-earth sesquisulfides (Ln = La, Nd, Sm, Gd) in the 3d core level region [91K]. The trivalence of Sm is testified by the value of the Sm 3d doublet line spin-orbit splitting (= 27.6 eV). E_b relative to E_F.

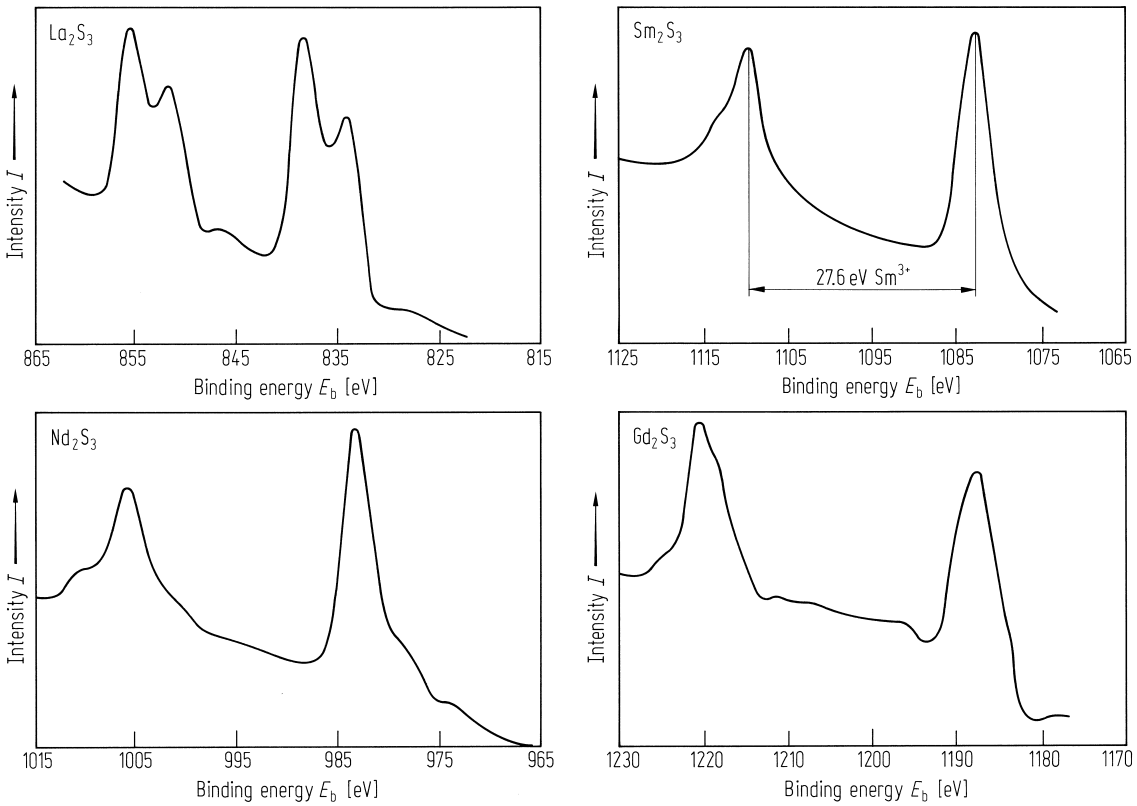

Fig. 9.

γ-Ln_2S_3. Electron loss spectra of the rare-earth sesquisulfides (Ln = La, Ce, Nd, Sm, Gd, Dy) for primary electron beam energy E_p = 750 eV. All the peaks, revealed from the second derivative d^2N/dE^2 are indicated by arrows [91K].

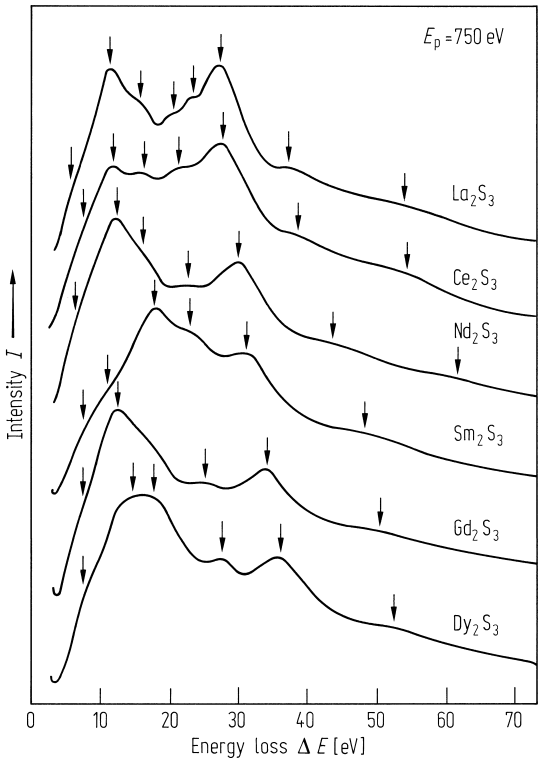

Fig. 10.

γ-La_2S_3; γ-Sm_2S_3. Reflection spectra [83B].

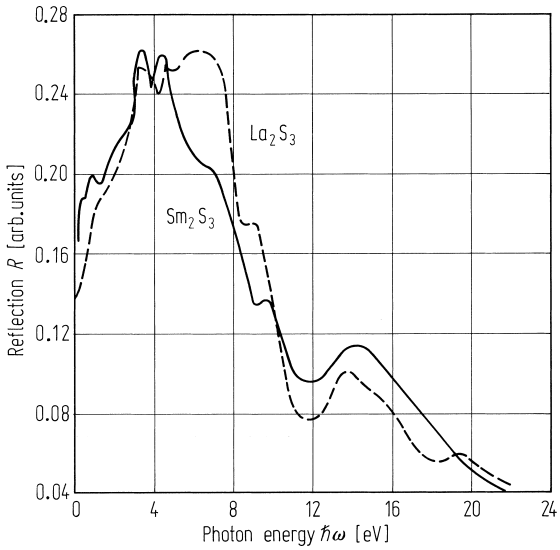

Fig. 11.

γ-Sm_2S_3. Dielectric constants and loss function vs. photon energy [83B].